Fuel Processing Technology 107 (2013) 138–146

Contents lists available at SciVerse ScienceDirect

Fuel Processing Technology

journal homepage: www.elsevier.com/locate/fuproc

LES of Delft-Jet-In-Hot-Coflow (DJHC) with tabulated chemistry and stochastic fields combustion model

Rohit Madhukar Kulkarni *, Wolfgang Polifke

Lehrstuhl für Thermodynamik, Technische Universität München, D-85747 Garching, Germany

ARTICLE INFO

Article history:
Received 17 March 2012
Received in revised form 11 June 2012
Accepted 12 June 2012
Available online 11 July 2012

Keywords:
MILD combustion
Tabulated chemistry
LES
Stochastic fields

ABSTRACT

In this work, a turbulent combustion model based on tabulated chemistry and stochastic fields model for turbulence chemistry interaction is applied to a lifted flame studied experimentally at Delft University, which emulates MILD combustion behavior. The experimental set-up consists of a jet of natural gas jet injected into a coflow of lean combustion products mixed non-uniformly with ambient air. The model used in this work has been extended to consider the non-homogeneous co-flow, by introducingan extra conserved scalar for the air stream. The model predicts the lift-off height satisfactorily and also captures the effect of reduced lift-off height with increasing jet Reynolds number. The LES results support the argumentation that the reason for the decrease in the lift-off height is due to enhanced entrainment of the vitiated co-flow into the jet, leading to increased reaction rates and lower autoignition delays. The combustion model shows potential to be used for MILD combustion regime and confirms its capability to be extended to multi-stream mixing cases. This feature makes the model suitable for complex industrial applications for low emission combustion.

1. Introduction

Combustion systems operating at low peak temperatures have been identified as an attractive alternative to conventional combustion systems in improving thermal efficiency and reduced pollutants [1]. The low-temperature combustion phenomenon, referred to as MILD (Moderate and Intense Low Oxygen Diluted) oxidation is achieved by preheating the oxidizer and reducing its oxygen content. This can be achieved by recirculating the burnt gases or in a sequential combustion system. Thetemperature is typically higher than the auto-ignition temperature. This reduced peak temperatures reduce NOx emissions. The combustion process in the MILD regime, where the reactivity of the mixture is reduced by low oxygen content, is kinetically controlled.

Cavaliere [2] gives a detailed review on the history, fundamentals and applications of MILD combustion. Out of various industrial application including furnaces in steel industry or HCCI engines, to name a few, one of the industrial examples related to power generation close to MILD combustion mode is the reheat combustor in Alstom GT 24/26 engine [2].

For the development of these applications, understanding of the MILD combustion in turbulent flows is important. Laboratory scale flames with vitiated co-flow with reduced oxygen content include: Cabra [3], Adelaide [4] and Delft [5,6] flame. The Cabra flame with 12% oxygen by mass in the coflow can be considered to be a border case for MILD combustion. The Adelaide flame and the Delft flame with 3–9% and 7–11% oxygen, respectively, can be considered to be definitely in the MILD combustion regime. The Delft flame, called DJHC (Delft Jet in Hot Coflow) from here on, is considered in this work.

The DJHC flame set up consists of jet of natural gas injected at high velocity into a coflow of burnt gases produced by a secondary burner. Measurements were carried out for various jet velocities. A decrease in the lift-off height was observed experimentally with an increase in the jet velocity. This makes the case important to study the interdependence of turbulence, mixing and chemistry in the MILD combustion regime. Another interesting feature of the DJHC flame is the non-uniform boundary conditions in the coflow. The oxygen content and the temperature in the co-flow are not uniform. In addition to these complexities, simulation of MILD combustion is in general a challenge for turbulent combustion models.

Coelho et al. [7] applied an Eulerian Particle Flamelet model (EPFM) in RANS to predict NO in the furnace studied by Plessing [8]. Kim et al. [9] used CMC to simulate the Adelaide burner [4]. Ihme et al. [10] extended the Flamelet Progress variable (FPV) model for the Adelaide burner. To consider the non-uniform co-flow an extra conserved scalar (mixture fraction) was used. The chemistry was tabulated by solving the laminar steady flamelet equation. A presumed Probability Density Function (PDF) approach was used for the turbulence-chemistry interaction. Beta PDF model was used for the mixture fractions (conserved scalars) and a Dirac function for the progress variable. De et al. [11] simulated the Delft flame in 2D with the EDC model [12] in RANS context with reduced methane

* Corresponding author.
E-mail address: kulkarni@td.mw.tum.de (R.M. Kulkarni).

0378-3820/$ – see front matter © 2012 Elsevier B.V. All rights reserved.
doi:10.1016/j.fuproc.2012.06.015

mechanisms. The EDC model captured the decreasing trend of lift-off height with jet Re number, but thelift-off heights predicted were too short and the temperatures were over predicted. The combustion model used in this work is based on tabulated chemistry and stochastic fields turbulence-chemistry interaction model. As combustion in MILD regime takes place at extremely lean conditions, where scalar dissipation rate is low and no reactive-diffusive structures exist, homogeneous reactors are used in this work to tabulate the chemistry. The advantage of this approach is its capability of being extended for multi-stream mixing cases, like the reheat combustor mentioned above, at a relatively low computational cost. LES have been performed for the DJHC flame for cases with lowest amount of oxygen in the co-flow at various jet Reynolds numbers for methane fuel. A case with different coflow temperature and oxygen content is also simulated to consider the effect of the changed Damköhler (Da) number, due to increased ignition delays. The remainder of the paper is organized as follows. The experimental setup is described first. The combustion model is then described along with its extension to multi-stream mixing cases. After a brief description of the numerical details, the results are compared with the experimental measurements followed by conclusions.

2. Test case

The test case in this work is the Delft Jet in Hot Coflow (DJHC) performed by Oldenhof et al. [5,6] at the Delft University. The design of the burner is similar to the Adelaide burner [4]. A jet of fuel enters into a coflow of hot air with low oxygen content. The high temperature ensures ignition of the injected fuel. The experimental setup consists of a primary burner and a partially premixed secondary burner. Fig. 1 shows the sketch of the flame. The diameter of the injector is 4.5 mm. The coflow is generated by an annulus secondary burner of 82.8 mm diameter upstream of the primary burner. It consists of a ring of premixed flames with air injected on both sides of the ring. The fuel tube is cooled using air stream. Due to the cooling air and the air injected along the secondary burner, the coflow at the inlet of the primary burner consists of a nonuniform profile of temperature and species.

The temperature and mass fraction of oxygen in the coflow at the inlet of the primary burner are shown in Fig. 2. Measurements were carried out for various coflow temperature and minimum oxygen mass fractions at the inlet. In this work the case with minimum amount of oxygen is considered for various jet Re numbers. Table 1 shows the boundary conditions for the fuel jet and the coflow. The velocity profiles for the cases are shown in Fig. 3.

Velocity and Temperatures were measured at 3, 15, 30, 60, 90, 120 and 150 mm downstream of the primary burner. Favre averaged velocities and Reynolds stresses were measured using Laser Doppler Anemometry (LDA). The temperature was measured using Coherent Anti-Stokes Raman Spectroscopy (CARS). The radial profile of oxygen concentration was measured using probe measurements.

Flame lift-off height was determined using chemiluminescence images obtained with intensified high speed camera. It was observed experimentally that the flame is stabilized by autoignition. Auto-ignition kernels appeared randomly and were convected downstream. The size of the kernels increased, while moving downstream. Interestingly,

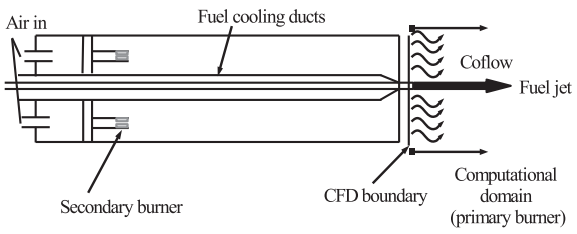

Fig. 1. Test case sketch.

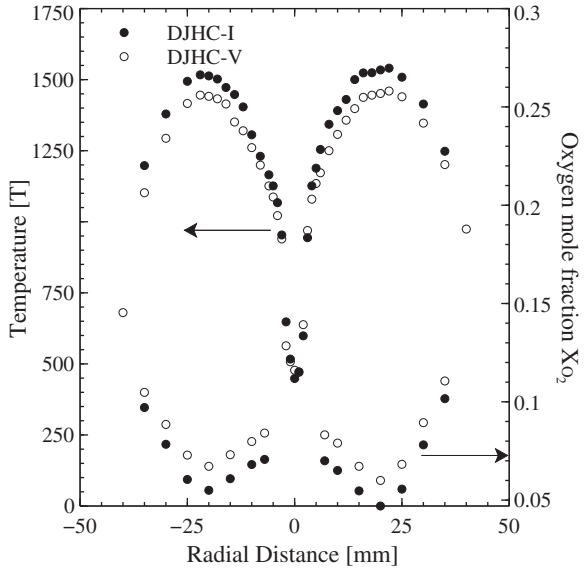

Fig. 2. Temperature and oxygen mole fractions at the boundary conditions for DJHC-I and DJHC-V.

but perhaps counter-intuitive with an increase in the jet velocity, the lift-off height was found to reduce. The lift-off height depended strongly on the co-flow temperatures.

3. Combustion model description

Before presenting the model formulation in detail, pertinent prior work is reviewed briefly. For turbulent premixed flames, Bradley and co-workers [13] suggested a “laminar flamelet model,” where the probability density function (”PDF”) of a reaction progress variable based on temperature rise is approximated by a beta function. Mean values of reaction progress and chemical species are obtained by integration over a detailed chemical kinetic laminar flame structure, weighted with the presumed PDF of the reaction progress variable. The influence of turbulent strain on meanreaction progress was taken into account by considering strained laminar flames and/or extinction at a critical strain rate [14]. In the mid-90s, this approach was used at ABB to model (partially) premixed combustion in gas turbines, including the case of non-homogeneous mixture fraction [15,16]. A similar approach for modeling autoignition under high pressure Diesel engine conditions was proposed by Chang et al. [17]. A flamelet library for the source term of the progress variable with 5 dimensions (progress variable, mixture fraction mean, mixture fraction variance, scalar dissipation rate and pressure) was built in the pre-processing step. The source term for the progress variable was weighted with the presumed beta-PDF shape of the reaction progress variable (CO_2).

The flamelet model with lookup-table was generalized to more than one progress variable by de Goey and co-workers [18], who coined the popular term “flamelet generated manifolds”. An adaptation to auto-ignition in a turbulent jet-in-cross-flow configuration, as it is found in reheat combustors, was proposed by Brandt et al. [19–21], with a progress variable based on intermediate species formed during the induction period. The lookup-table was built

Table 1
Simulated cases.

Case	Re_j	$T_{co,max}$ [K]	$T_{co,min}$ [K]	$X_{co,min}$ [−]	$X_{co,av}$ [−]	T_f
DJHC-I	4100	1540	695	0.055	0.076	430
DJHC-I	8800	1540	695	0.055	0.076	460
DJHC-V	4600	1460	695	0.066	0.088	380

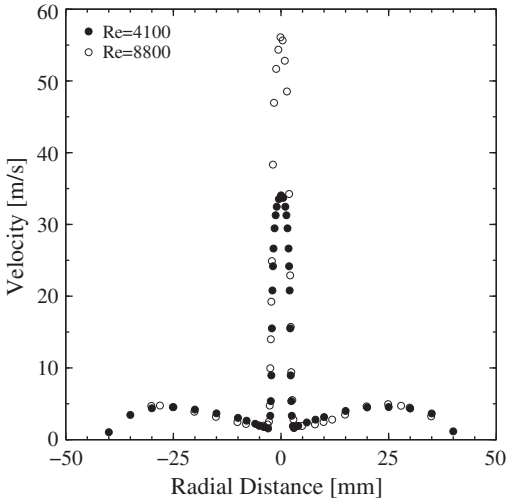

Fig. 3. Velocity boundary conditions for the DJHC-I (Re = 4100 and 8800). DJHC-V velocity boundary conditions are same as DJHC-I with Re = 4100.

from 0D reactors with detailed chemistry, rather than reactive-diffusive structures. For large eddy simulation of partially premixed or non-premixed flames, formulations based on progressvariable and mixture fraction were proposed by Pierce and Moin [22,23] and Vervisch and co-workers [24–26].

In the present paper, the model of Brandt et al. [19–21] is developed further. Firstly, a progress variable based on a combination of intermediate and final product species is introduced, such that it describes both the build-up of radical species during the induction period and the subsequent heat release. Secondly, following [27] the stochastic fields turbulence chemistry interaction model is implemented in the LES context. The major advantage of the stochastic fields model is that it can be easily extended to multiple-stream mixing cases avoiding the problems of modeling the second order moments and the presumed shape of the PDF. The computational cost is reduced due to the tabulated chemistry. The elements of the model, viz. the chemistry tabulation and the turbulence chemistry interaction are described in the next two sub-sections.

3.1. Chemistry tabulation

The present work used the tabulation method based on perfectly mixed homogeneous reactors as it includes the slow chemistry necessary for partially premixed cases. The open source code CANTERA [29] has been used to tabulate the chemistry. The homogeneous reactors march in time. The following system of ODEs (Ordinary Differential Equations) are solved by the chemical kinetics code ([29] in this work)

$$\rho\frac{\partial\phi_i}{\partial t}=\dot{\omega}_i \tag{1}$$

where $\phi_i=\{Y_i, h\}$. Initial conditions of the reactors are imposed as a function of the mixture fraction given by:

$$\phi_i^{t=0}=\phi_{i,oxidizer}+Z\left(\phi_{i,fuel}-\phi_{i,oxidizer}\right) \tag{2}$$

During the evolution of the reactors, the rate of change of the progress variable is tabulated as a function of the progress variable. The tabulation points are clustered close to large gradients (rapid increase) in the progress variable. Along with this the source terms for various species of interest and the heat release is also tabulated.

A combination of an intermediate species and a product should be used as the progress variable. Domingo et al. [26] used CO and CO2 as a suitable progress variable for Cabra flame [3]. Fig. 4 shows the evolution of CH_2O, CO and CO_2 for a homogeneous reactor with most reactive mixture fraction ($Z_1=0.01$) for the present DHJC case. The ignition delay time for this mixture fraction is about 1.9 ms. During initial stages of evolution (until 1 ms), the mass fraction of CH_2O is order of magnitudes higher than CO. The inclusion of CH_2O in the progress would not have a major impact on the results in case of relatively high oxygen contents like the Cabra flame. But, in flameless combustion, due to the reduced oxygen content in the coflow, the pre-ignition chemical reactions are slower (lower Damköhler number). Therefore,it is recommended to include CH_2O in the progress variable definition. In this work, $CH_2O+CO+CO_2$ has been used as the progress variable. In Section 4, the sensitivity of the lift-off height with different progress variables is described.

3.2. Stochastic fields

As the chemistry is not resolved in the LES, the non-linear chemical source term for the reactive scalar, the progress variable in the present work, needs closure. Two known approaches exist for the closure of this term, viz. the presumed and the transported PDF method. The presumed PDF method was used successfully by [26,28]. The approach used in this work is the transported PDF based on Eulerian formulation [27]. This method of the turbulence-chemistry interaction is also known as the Eulerian Monte Carlo method. The advantage of the transported PDF methods is the closed chemical source term. There are two approaches proposed by Valino [27] and Sabelnikov [30] based on the Ito and Stratonovitch calculus, respectively. The formal formulation based on Ito calculus is used in this work. The model is based on a system of stochastic differential equations equivalent to to the joint PDF evolution equations. The 'stochastic fields' are continuous and twice differentiable in space and non-differentiable (white) in time. A number of fields are used to describe the possible sub-grid realizations. The statistical error reduces with number of fields. In LES, as argued in [31–34], few number (about 8) of fields is necessary in LES. To be consistent as far as the turbulence-chemistry interaction model,8 fields have been used in this work.ewline The application of the combination of this turbulence-chemistry interaction with tabulated chemistry for lifted flames is the novelty of this work. Instead of solving the stochastic partial differential equations for all the chemical species, the PDEs are solved for the mixture fraction and

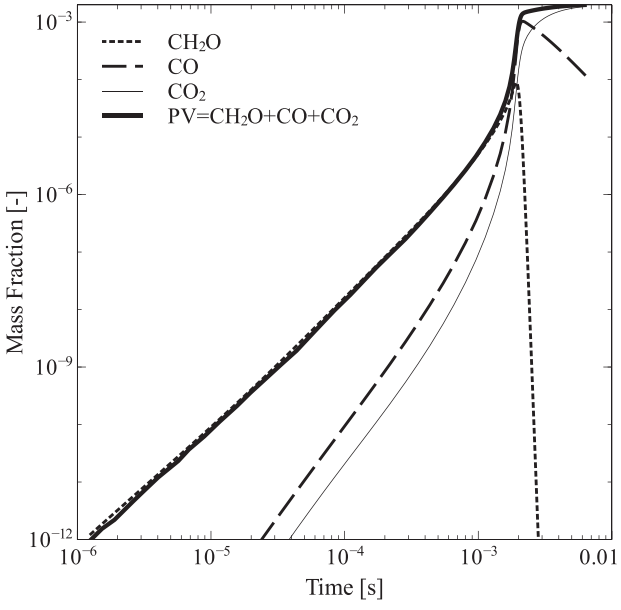

Fig. 4. Important species evolution for the most reactive mixture fraction $Z_1=0.01$.

the progress variable. The PDEs solved in the model are described in Eqs. (1) and (2).

$$\bar{\rho}\frac{dZ^n}{dt} = -\bar{\rho}\tilde{u}_i\frac{dZ^n}{dx_i} + \bar{\rho}\frac{d}{dx_i}\left[(D_l + D_t))\frac{dZ^n}{dx_i}\right] + \bar{\rho}(2(D_l + D_t))^{1/2}\frac{dZ^n}{dx_i}\frac{dW_i^n}{dt} - \frac{\bar{\rho}}{2\tau_{sgs}}\left(Z^n - \tilde{Z}\right) \quad (3)$$

$$\bar{\rho}\frac{dY_c^n}{dt} = -\bar{\rho}\tilde{u}_i\frac{dY_c^n}{dx_i} + \bar{\rho}\frac{d}{dx_i}\left[(D_l + D_t))\frac{dY_c^n}{dx_i}\right] + \bar{\rho}(2(D_l + D_t))^{1/2}\frac{dY_c^n}{dx_i}\frac{dW_i^n}{dt} - |\frac{\bar{\rho}}{2\tau_{sgs}}\left(Y_c^n - \tilde{Y_c}\right)dt + \bar{\rho}\dot{\omega}_c^n(Z^n, Y_c^n) \quad (4)$$

The first and the second term on the right hand side of the equations are the convective and diffusive terms, respectively. The third term on the right hand side is the stochastic term. The stochastic term depend on the effective diffusivity, gradient of the scalar and the Wiener term. The Wiener term is approximated by time-step increments $dt^{1/2}\eta_i$, where η_i is a dichotomous random number. The dichotomous random number η_i [−1,+1] is different in different directions, but is same for a particular field for all the scalars. The random number is different for different fields. One of the restrictions on the random numbers is that the sum of all the random numbers in a direction should sum up to 0. The fourth term is the micro-mixing model. The one used in this work is the IEM (Interaction by Exchange with the Mean) model. The sub-grid time scale $\tau_{sgs} = \left(\frac{\mu+\mu_{sgs}}{\bar{\rho}\Delta^2}\right)^{-1}$. The stochastic fields $Z^n(x, t)$ correspond to an equivalent stochastic system of one-point PDFs. The last term in Eq. (2) is the chemical source term for the progress variable. This term is absent in the mixture fraction PDE as the mixture fraction is a conserved scalar. The source term of the progress variable is a function of the mixture fraction and the progress variable of that particular field.

The fields can be used to represent the density-weighted sub-grid PDF of the scalar (mixture fraction in Eq. (3) by

$$P_{sgs}(Z; x, t) = \frac{1}{N}\sum_{n=1}^{N}\delta[Z - Z^n(x, t))] \quad (5)$$

The evaluation of the first order moment (mean) can be done by

$$\tilde{Z} = \frac{1}{N}\sum_{n=1}^{N}Z^n \quad (6)$$

The source terms for the species and the energy equation solved in LES can be calculated from

$$\tilde{\dot{\omega}_\alpha} = \bar{\rho}\frac{1}{N}\sum_{n=1}^{N}\dot{\omega}_\alpha^n(Z^n, Y_c^n) \quad (7)$$

Model assumptions may be summarized as follows:

1. Reaction progress is described by a composite progress variable Y_c. For the case of methane autoignition, the progress variable is based on concentrations of intermediates CH_2O, CO and product species CO_2.
2. No thin reaction–diffusion structures are formed during the induction period [35,36], thus a direct impact of strain rate or scalar dissipation on reaction progress is neglected. Tabulation is consequently based on homogeneous reactor data.
3. Differential and preferential diffusion effects are not considered.

3.3. Extension of the model for ternary mixing

To consider the non-uniform boundary condition due to the burnt gases from the secondary burner mixed with air, an extra conserved scalar was used in addition to the one used for the fuel. The mixture fraction Z_1 was used for the fuel stream and Z_2 for the air stream. At any location the sum of the mixture fraction subtracted from 1 gives the amount of hot gas. The Z_2 boundary condition is located at the jet radius if 2.25 mm. The maximum temperature and the minimum oxygen concentration in the co-flow were considered as boundary conditions for the hot gas.

At the boundary conditions the additional mixture fraction Z_2 is calculated as a function of the temperature. Eq. (6) describes the method of calculating the second mixture fraction at the inlet:

$$Z_2 = \frac{T_{co,max} - T}{T_{co,max} - T_{air}} \quad (8)$$

The assumption behind this equation is that the oxygen concentration and temperature are correlated, which is true closer to the axis. But, this is not necessarily true for the outer part of the co-flow due to wall and radiation heat losses. These effects are neglected in this work. These effects can be included by introducing an extra dimension (e.g. enthalpy) in the look-up table. Tabulation is done for various combinations of the two mixture fractions with the constraint that the summation of the two mixture fraction is less than one, leading to a triangular zone for the tabulated region. Fig. 5 shows the mixture fraction triangle.

The initial conditions (reactant mass fractions and enthalpy) for the homogeneous reactors are calculated using:

$$\phi_i^{t=0} = Z_1 * \phi_{i,Z_1} + Z_2 * \phi_{i,Z_2} + (1 - Z_1 - Z_2) * \phi_{i,Z_3} \quad (9)$$

In LES, stochastic fields for the mixture fractions Z_1 and Z_2 and the progress variable are solved. Eq. (1) is valid for both the mixture fractions.

$$\bar{\rho}\frac{dZ_1^n}{dt} = -\bar{\rho}\tilde{u}_i\frac{dZ_1^n}{dx_i} + \bar{\rho}\frac{d}{dx_i}\left[(D_l + D_t))\frac{dZ_1^n}{dx_i}\right] + \bar{\rho}(2(D_l + D_t))^{1/2}\frac{dZ_1^n}{dx_i}\frac{dW_i^n}{dt} - \frac{\bar{\rho}}{2\tau_{sgs}}\left(Z_1^n - \tilde{Z_1}\right) \quad (10)$$

$$\bar{\rho}\frac{dZ_2^n}{dt} = -\bar{\rho}\tilde{u}_i\frac{dZ_2^n}{dx_i} + \bar{\rho}\frac{d}{dx_i}\left[(D_l + D_t))\frac{dZ_2^n}{dx_i}\right] + \bar{\rho}(2(D_l + D_t))^{1/2}\frac{dZ_2^n}{dx_i}\frac{dW_i^n}{dt} - \frac{\bar{\rho}}{2\tau_{sgs}}\left(Z_2^n - \tilde{Z_2}\right) \quad (11)$$

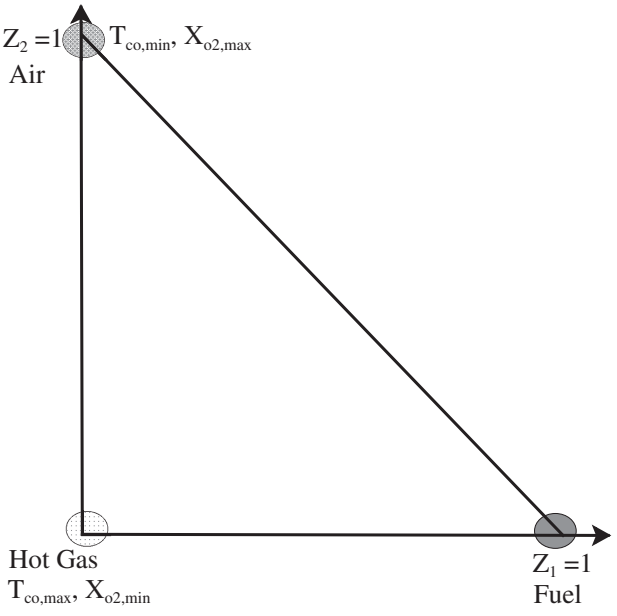

Fig. 5. Tabulation triangle with boundary condition.

Eight number of fields are used in this work. Each field carries a reactive scalar, i.e. the progress variable, in addition to the conserved mixture fractions. The source term for the progress variable in Eq. (2) is then a function of the mixture fractions and the progress variable for a particular field $\bar{\rho}\dot{\omega}_c^n(Z_1^n, Z_2^n, Y_c^n)$. The equation would be:

$$\begin{aligned}\bar{\rho}\frac{dY_c^n}{dt} &= -\bar{\rho}\tilde{u}_i\frac{dY_c^n}{dx_i} + \bar{\rho}\frac{d}{dx_i}\left[(D_l + D_t))\frac{dY_c^n}{dx_i}\right] \\ &+\bar{\rho}(2(D_l + D_t))^{1/2}\frac{dY_c^n}{dx_i}\frac{dW_i^n}{dt} - \frac{\bar{\rho}}{2\tau_{sgs}}\left(Y_c^n - \tilde{Y}_c\right)dt \\ &+\bar{\rho}\dot{\omega}_c^n(Z_1^n, Z_2^n, Y_c^n)\end{aligned} \tag{12}$$

The filtered source terms for the species and heat release will also be a function of the mixture fractions and the progress variable given by Eq. (7).

$$\widetilde{\dot{\omega}}_\alpha = \bar{\rho}\frac{1}{N}\sum_{n=1}^{N}\dot{\omega}_\alpha^n(Z_1^n, Z_2^n, Y_c^n) \tag{13}$$

The chemical source term for the progress variable is thus closed avoiding the problem of modeling the higher order moments of the mixture fraction and the multi-dimensional PDF, which is necessary in presumed PDF approach. Also, the fluctuations of the progress variable are considered.

4. Numerical details

The look-up table was generated using the boundary conditions described below in Table 1 using Cantera. The GRI30 chemical mechanism was used. The look-up table had about 41 points non-uniformly distributed in the two mixture fraction directions. About 80 points were used in the progress variable direction. The table size was 8 MB and the tabulation time was approximately 30 min with a 2.5 GHz QuadCore computer.

The LES simulations were performed using FLUENT. The Smagorinsky dynamic model was used for the subgrid eddy viscosity. Adiabatic no-slip boundary conditions are used at the walls. The laminar and turbulent Schmidt numbers had a constant value of 0.7 and 0.9, respectively, for all the species and scalars (mixture fraction and progress variable).

The simulation time for a single run was 10 days on a 16 core computer. The simulations were carried out with a time stepping of 2e-6 s, which ensures a CFL < 0.7.

Table 1 shows the boundary conditions for the cases considered in this work. The temperature and oxygen content at the boundary conditions are shown in Fig. 2.

Fig. 2 shows that with an increase in the temperature, the oxygen percentage is also reduced correspondingly. On one hand the increase in temperature will promote reactions, while the reduction in oxygen content will hinder them. Those two effects will counteract each other. Depending on which one of them is dominating, the lift-off length will change. The combustion model has to consider these effects along with the mixing between hot gases and air in the co-flow. The velocities for the Re = 4100 and Re = 8800 cases are shown in Fig. 3. The velocity boundary conditions for the DJHC-V case are the same as that of the DJHC-I with Re = 4100.

5. Results

5.1. Grid independence

In partially- or non- premixed cases the flow field and mixing between different streams is extremely important, as the chemical reactions strongly depend on the mixing processes. In the MILD combustion regime, where the Da number is low, combustion is kinetically controlled. Auto-ignition takes place in very lean conditions due to reduced oxygen content in the co-flow. The chemical reactions are strongly affected by the turbulent co-flow. The turbulence-chemistry interaction plays a major role in MILD combustion regime. Therefore, proper prediction of flow and mixing is an absolute necessity for successful combustion simulation.

The test case with Re = 8800 has been considered as a representative for the grid independence study, due to its highest jet velocity (Reynolds number). A coarse mesh with 750 thousand and a fine mesh with 1 million cells was considered. The simulations were carried out with the combustion model described above.

Various mesh quality indicators have been proposed in the literature. The aim of LES is to solve for the large scales of the size of integral length scale. According to Pope [37], in a good LES, 80% of the kinetic energy should be resolved. Based on this criteria various quality indicators were proposed by Celik [38]. One of the them is considered here for the mesh quality.

To study the LES mesh quality, two meshes with different sizes were used. Mesh 1 comprises of 150x70x48 nodes in axial, radial and azimuthal directions respectively. The corresponding number of nodes for a finer mesh, Mesh 2, are $200\times90\times56$. The mesh was clustered towards the central axis in order to resolve the mixing layer between the fuel and the air stream. DJHC-I with Re = 8800 boundary conditions were used for this study due to the highest jet Reynolds number. The following LES quality index suggested by [38] based on the viscosity ratio has been used for the study:

$$\text{LES\_}IQ = \frac{1}{1 + 0.05\left(\frac{\nu_{t,eff}}{\nu}\right)^{0.53}} \tag{14}$$

In Eq. (14), $\nu_{t,eff}$ is the effective viscosity (laminar + turbulent) and ν is the molecular viscosity. The larger the modeled viscosity, the lower will be the quality criteria. With an improvement in the mesh quality, the ratio increases and in an extreme case attains a value of 1. According to [38], the LES quality index should be above 0.8 for quality LES mesh. The quality criteria for both the meshes is shown in Fig. 6. The LESquality factor is satisfied by both the meshes. The quality of the finer mesh is obviously better.

The velocity field was measured using LDA technique radially at various axial distances. The resolved velocity for both the meshes is compared with the experimental measurements in Fig. 7. Fig. 8 does the same for turbulent kinetic energy.

From the velocity and the turbulent kinetic energy profiles for the two meshes at various downstream locations shown in Figs. 7 and 8, respectively, it can be safely said that both the meshes are satisfactory for good LES. The coarser mesh with 0.65 million cells is used for the simulations from this point.

5.2. Velocity and Mixing Field

The combustion process in MILD combustion is kinetically controlled. The chemical reactions are a strong function of the mixing between fuel, air and hot gas. The success of any combustion model depends on the quality of flow and mixing field. In this sub-section the velocities from the LES simulations are compared with the experimental measurements. Figs. 9 and 7 shows the radial velocity distribution at various axial locations for DJHC-I at Re numbers of 4100 and 8800, respectively.

A satisfactory velocity distribution is obtained in the LES. Fig. 10 compares the Z_2 mixture fraction for the cases studied in this work. A line showing the stoichiometric mixture fraction $Z_{1,st} = 0.02$ is also shown . The distribution of Z_2 on the iso-line of $Z_{1,st}$ is important, as the reactions are fastest at mixture fraction close tho this value for a given Z_2. A lower value of $Z2$ will mean a higher amount of hot gas at that location. The hot gas accelerates the chemistry due to the higher temperature. The distribution of Z_2 for DJHC-I 4100 and DJHC-V 4500

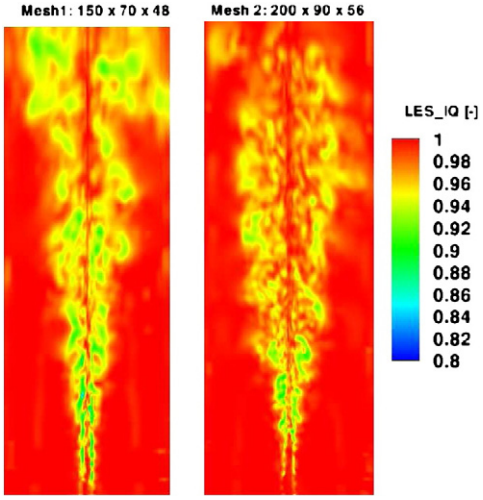

Fig. 6. LES quality criteria, Mesh 1: 150×70×48 and Mesh 2: 200×90×56 nodes in axial, radial and azimuthal directions, respectively.

are quite similar due to similar jet Re numbers. For DJHC-I with Re = 8800, lower amount of Z_2 is observed in comparison to the other two cases. This is because of the faster entrainment of the hot gases into the jet. This was also observed in the RANS simulation of De et al. [11] This point is discussed at length in [6]. The enhanced entrainment should lead to faster chemistry and lower lift-off height. This is the point of discussion in Section 5.

5.3. Temperature distribution

The temperature distribution for the DJHC-I cases with Re = 4100 and 8800 are shown in Fig. 11. In Fig. 11, an additional line for the mixing temperature (without combustion) is also plotted for reference. At downstream locations greater than 30 mm, a larger discrepancy is observed between LES temperature (both with and without combustion) and the measured temperature close to the walls. This might be due to the radiation or wall heat losses, which are not

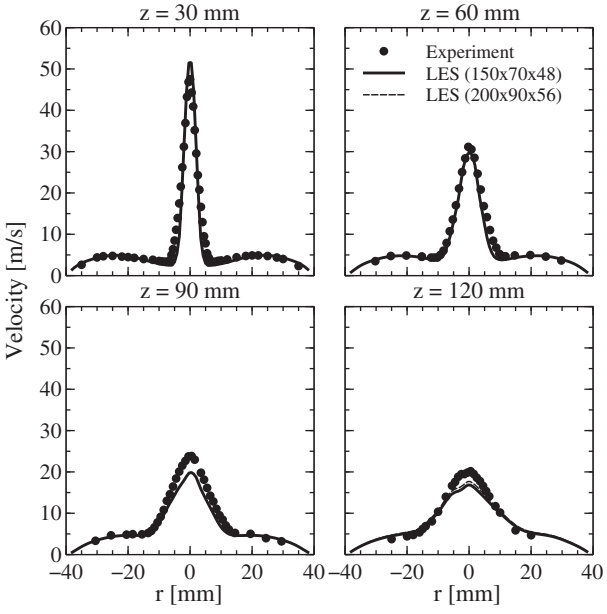

Fig. 7. Radial velocity distribution for DJHC-I Re = 8800 at various downstream locations. Mesh 1: 150×70×48 and Mesh 2: 200×90×56 nodes in axial, radial and azimuthal directions, respectively.

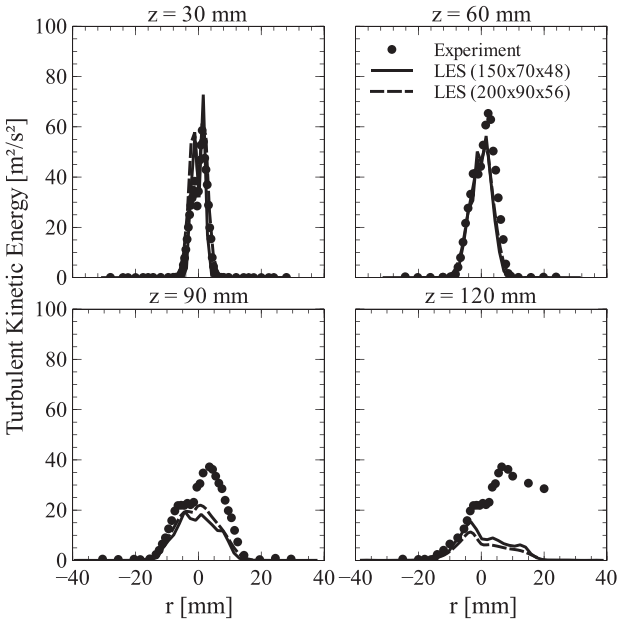

Fig. 8. Radial distribution of the turbulent kinetic energy for DJHC-I Re = 8800 at various downstream locations. Mesh 1: 150×70×48 and Mesh 2: 200×90×56 nodes in axial, radial and azimuthal directions, respectively.

considered in the simulation. The discrepancies might also be contributed to measurement error. Also in the work done by De et al. [11], a large discrepancy in temperature was observed between the measured and RANS results. This was contributed to a lower lift-off height predicted by the EDC model.

The lines with and without combustion are indistinguishable for a length of 30 and 60 mm downstream of the nozzle. An increase in the temperature is observed from 90 mm onwards. This indicates that the flame is stabilized between 60 and 90 mm downstream the nozzle. Determining the lift-off height is the topic of next sub-section. The temperature measurements overall show a good agreement with the measured temperatures close to the axis. It is interesting to observe from the difference between the LES curves with and without combustion that a very

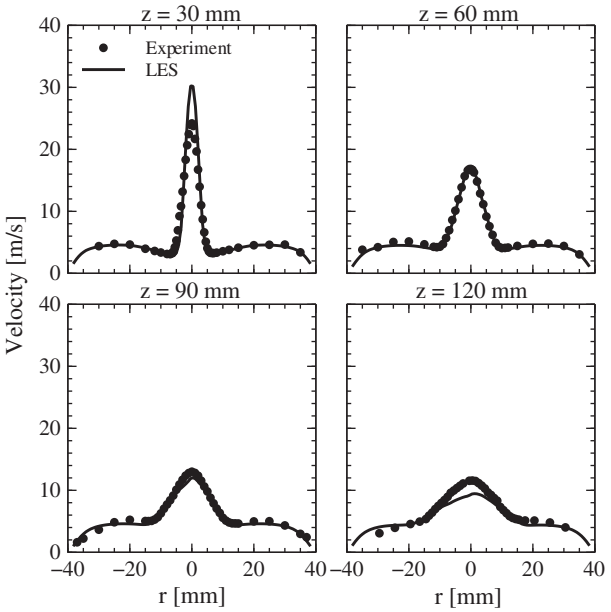

Fig. 9. Radial velocity distribution for DJHC-I Re = 4100 at various downstream locations.

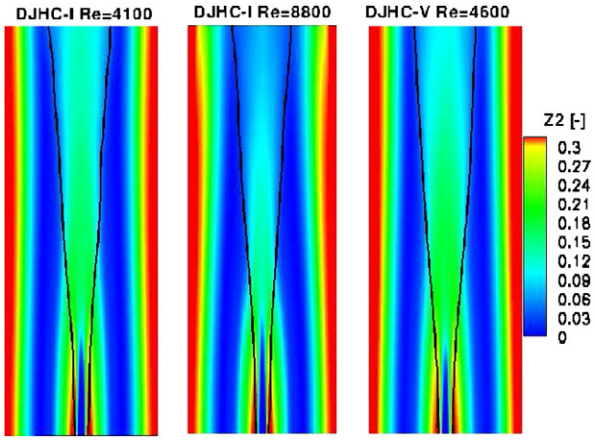

Fig. 10. Time averaged air mixture fraction distribution at the central cross section. Line: Most reactive fuel mixture fraction.

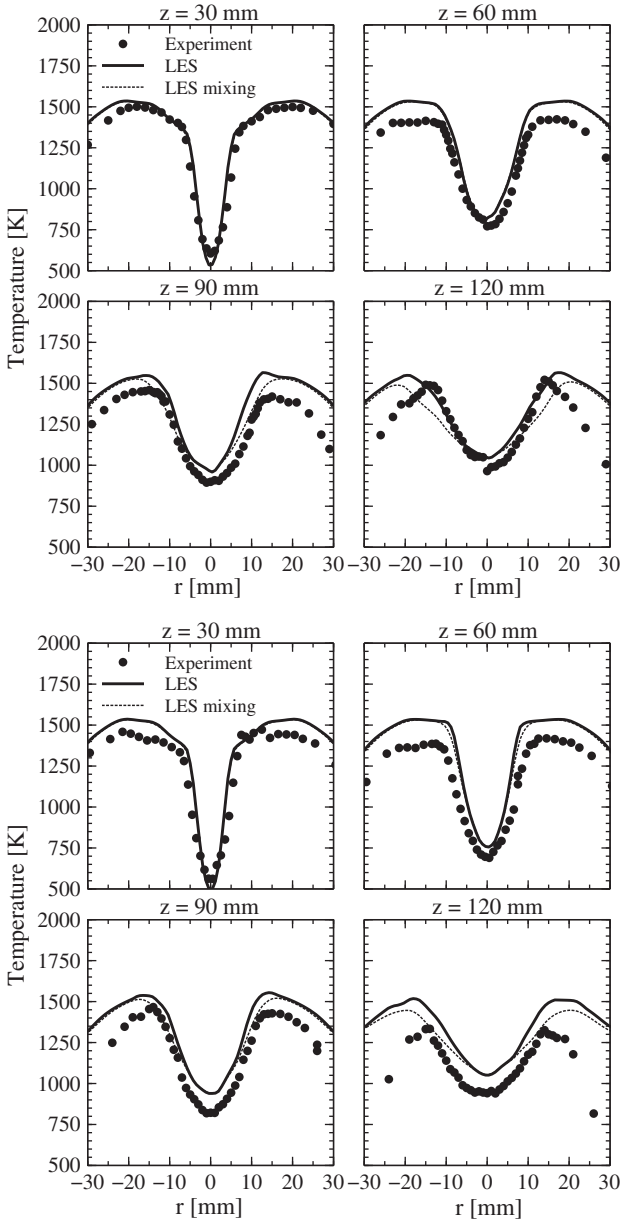

Fig. 11. Radial temperature distribution for DJHC-I Re = 4100 (top) and Re = 8800 (bottom) at various downstream locations.

low amount of heat is released compared compared to traditional combustion systems. No significant over prediction is observed. This shows the capability of the model to capture the slow chemistry or kinetically controlled combustion processes in MILD regime.

5.4. Sensitivity to the progress variable definition

The progress variable is not a physical quantity, but a helping variable that describes the progress of the reactions. The definition of the progress variable is important for the success of the combustion model. As described in Section 1, $CO + CO_2$ is generally used as a progress variable. The curves in Fig. 4 show that a significant amount of CH_2O is produced before CO in the initial stages of a reactor evolution. In this subsection, the sensitivity of the LES combustion model to the progress variable definition will be investigated. Fig. 12 shows the OH mass fraction contour for three different definitions of the progress variable.

Generally, an OH mass fraction of 1e-3 is considered as a criteria for ignition. The difference in the lift-off heights can clearly be seen. The lift-off length of about 85 mm can be seen with the inclusion of CH_2O in the progress variable definition, which is close to the experimental value. The error in the lift-off height using CO_2 as a progress variable is significant. There is also a considerable difference between the progress variable with and without CH_2O. The error is expected to increase with still lower temperatures or oxygen content. The reason for this, as described earlier, is due to the reduced pre-ignition chemical reactions that lead to a considerable difference in the CH_2O and CO evolution (refer Fig. 4). For the cases described in Table 1, a composite progress variable with CH_2O, CO and CO_2 will be used in the following sections.

5.5. Lift-off Height

For the prediction of lift-off height, various criteria are available in literature. In many of the measurements OH chemiluminescence has been considered as an indicator of heat release and therefore the lift-off height. In various simulation works related to lifted flames, lift-off heights based on an increase in the temperature over mixing temperature [26], OH mass fraction [39] has been used. In the experimental work by Oldenhof et al. [11] on the DJHC flame, the lift-off height was based on a different approach.

The lift-off height was related to the probability of the presence of flame pockets. A flame pocket is defined where an OH mass fraction attained a value of 1e−3. Two different flame probabilities were defined., Pb_1 and Pb_2. $Pb_1(z)$ is the probability of finding a flame pocket anywhere on a radial line stretching outward from the burner axis as a function of the axial height. The second probability $Pb_2(z)$ is that of finding a flame pocket at a certain axial height. The probability Pb_1

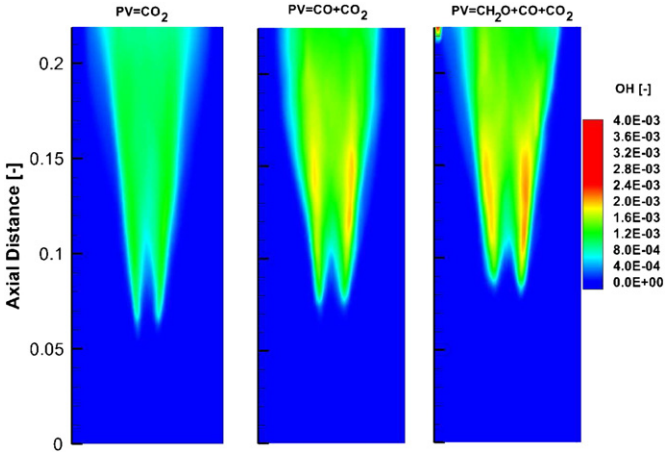

Fig. 12. Time averaged OH mass fraction distribution for three different progress variables.

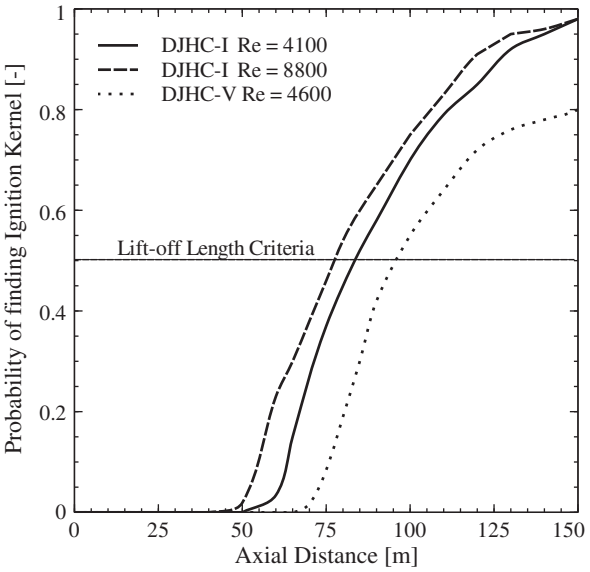

Fig. 13. Probability distribution of ignition kernels over the tube length.

has been used in this work. In this method, a location with OH signal at any radial distance was assigned a probability of 1. For each location, the number of counts where a burning location was found was divided by a total number of images, producing a flame probability P_{b1}. As suggested by Oldenhof et al. [6], a $Pb_1 = 0.5$ is defined as the lift-off height. Fig. 13 shows the probability Pb_1 for the cases studied in this work over the axial length. Thetime averaged axial distribution of OH mass fraction is shown in 14.

Figs. 13 and 14 show clearly an increase in the lift-off height for an increase in the jet Re number for DJHC-I case. This observation is due to the faster mixing between the hot gases and the jet, which promotes reactions and reduces the auto-ignition length. This observation is in agreement with the previous works of De et al. [11]. With reduced coflow temperature (DJHC-V) with a similar Re number, the autoignition length increases. This effect is expected due to the reduced reaction rates or increased ignition delays with reduced temperatures. Table 2 compares the experimentally observed lift-off heights with those from the LES simulations.

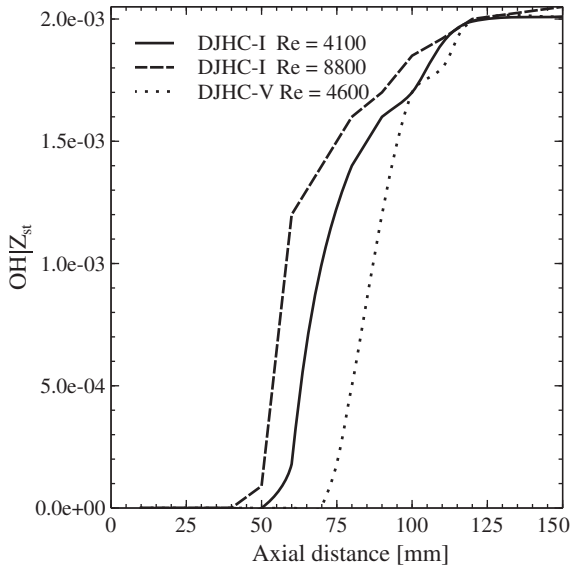

Fig. 14. Time averaged OH mass fraction conditioned on the most reactive mixture fraction.

Table 2
Mean lift-off heights.

Case	Experimental [mm] [6]	LES [mm]
DJHC-I $Re_j = 4100$	80	85
DJHC-I $Re_j = 8800$	78	78
DJHC-V $Re_j = 4600$	100	95

Fig. 15 shows the snapshots and the time averaged OH mass fraction distribution for the cases. The trend in the lift-off height is clearly visible in the snapshots and the time averaged OH mass fractions in Fig. 15. These results show the capability of the proposed model of tabulated chemistry and stochastic fields turbulence chemistry interaction to consider cases with multi-stream mixing. The extension of the model in this respect, without the need for any additional model complexities or assumptions, is the major advantage of the approach over the presumed PDF methods.

6. Conclusion

A combustion model based on tabulated chemistry based on reactors and stochastic fields turbulence-chemistry has been validated for a lifted-flame in MILD combustion regime with multi-stream mixing. The model satisfactorily predicted the lift-off height for different jet velocities and co-flow temperatures. The model correctly predicted the trend of decreasing lift-off height with jet velocity due to the enhanced entrainment of the hot gases into the jet. The extension of the model to multi-stream mixing cases without any additional modeling assumptions or complexities is the major advantage of the approach, which makes it suitable for complex industrial applications. The model has a potential for further extension to include wall heat losses by introducing an enthalpy dimension in the look-up table.

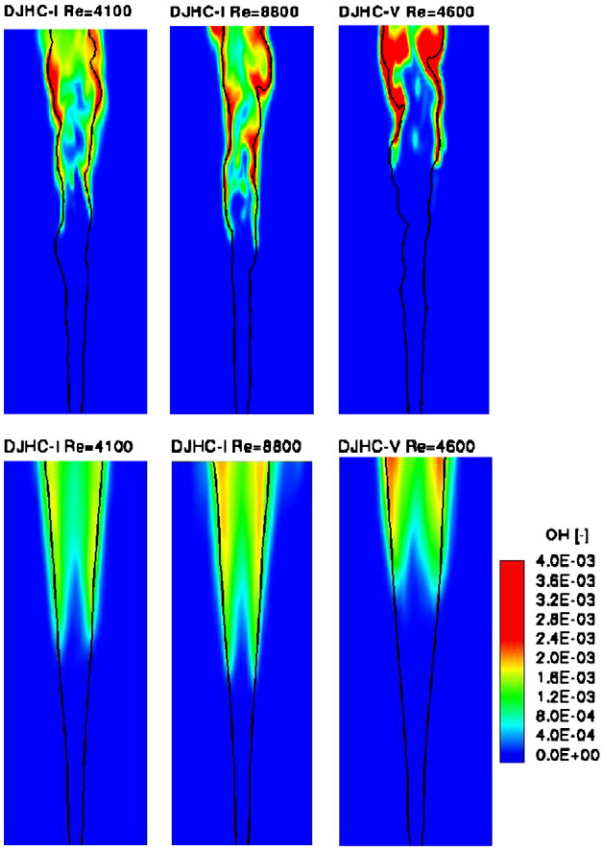

Fig. 15. OH mass fraction distribution. Top: Snapshot Bottom: Time averaged. Isoline: Most reactive mixture fraction ($Z_1 = 0.01$).

Acknowledgement

Financial support for this work has been provided by Alstom Power, coordinated by Uwe Ruedel. Fruitful discussions with Birute Bunkute, Michael Düsing, Fernando Biagioli, and Bruno Schuermans (Alstom) and Patrick Jenny (ETH Zürich) are gratefully acknowledged. Our special thank goes to Dirk Roekaerts and Michael Stollinger (Delft University) for providing the experimental data.

References

[1] J. Wünning, J.G. Wünning, Flameless oxidation to reduce thermal no-formation, Progress in Energy and Combustion Science 23 (1997) 81–94.
[2] A. Cavaliere, M. de Jaonnon, Mild combustion, Progress in Energy and Combustion Science 30 (2004) 329–366.
[3] R. Cabra, J.Y. Chen, A.N. Dibble, R.S. Barlow, Lifted methane-air jet flames in a vitiated coflow, Combustion and Flame 143 (2005) 491–506.
[4] B. Dally, A. Karpetis, R. Barlow, Structure of turbulent non-premixed jet flames in a diluted hot coflow, In: Proceedings of the Combustion Institute, 2002.
[5] E. Oldenhof, M. Tummers, E. van Veen, D. Roekaerts, Ignition kernel formation and lift-off behaviour of jet-in-hot-coflow flames, Combustion and Flame 157 (2011) 1167–1178.
[6] E. Oldenhof, M. Tummers, E. vanVeen, D. Roekaerts, Role of entrainment in the stabilisation of jet-in-hot-coflow flames, Combustion and Flame 158 (2011) 1553–1563.
[7] P. Coelho, N. Peters, Numerical simulation of a mild combustion burner, Combustion and Flame 124 (3) (2001) 503–518.
[8] T. Plessing, W.J.G. Peters, Laseroptical investigation of highly preheated combustion with strong exhaust gas recirculation, Proceedings of the Combustion Institute 27 (1998) 503–518.
[9] S.H. Kim, K. Huh, B. Dally, Conditional moment closure modeling of turbulent nonpremixed combustion in diluted hot coflow, Proceedings of the Combustion Institute 30 (2005) 751–757.
[10] M. Ihme, Y.C. See, flamelet modeling of three-stream mild combustor: Analysis of flame sensitivity to scalar inflow conditions, Proceedings of the Combustion Institute 33 (2011) 1309–1317.
[11] A. De, E. Oldenhof, P. Sathiah, D. Roekaerts, Numerical simulation of delft-jet-in-hot-coflow (djhc) flames using the eddy dissipation concept model for turbulence-chemistry interaction, Flow, Turbulence and Combustion 1386–6184 (2011) 1–31.
[12] B. Magnussen, B. Hjertager, On mathematcal modeling of turbulent combustion with special emphasis on soot formation and combustion, Proceedings of the Combustion Institute (1976) 719–729.
[13] D. Bradley, L.K. Kwa, A.K.C. Lau, Laminar flamelet modelling of recirculating premixed methane and propane-air combustion, Combustion and Flame 71 (1998) 109–122.
[14] D. Bradley, A. Lau, The mathematical modelling of premixed turbulent combustion, Pure and Applied Chemistry 62 (5) (1990) 803–814.
[15] A.C. Benim, K.J. Syed, Laminar flamelet modelling of turbulent premixed combustion, Applied Mathematical Modelling 22 (1998) 113–136.
[16] W. Polifke, M. Bettelini, W. Geng, M. U. C., W. Weisenstein, P. Jansohn, Comparison of combustion models for industrial applications, In: Eccomas 98, Athens, Greece, 1998.
[17] C. Chang, Z. K. N., B. K.N.C., B. Rogg, Modelling and simulation and autoignition under simulated diesel engine conditions, Combustion Science and Technology 113–114 (1996) 205–219.
[18] L. De Goey, J. ten Thije Boonkkamp, A flamelet description of premixed laminar flames and the relation with flame stretch, Combustion and Flame 119 (3) (1999) 253–271.
[19] M. Brandt, W. Polifke, B. Ivancic, P. Flohr, P. B., Auto-ignition in a gas turbine burner at elevated temperature, In: International Gas Turbine and Aeroengine Congress & Exposition, ASME, 2003, (2003-GT-38224), Atlanta, GA, U.S.A. (2003).
[20] B. Ivancic, P. Flohr, B. Paikert, M. Brandt, W. Polifke, Auto-ignition and heat release in a gas turbine burner at elevated temperature, In: International Gas Turbine and Aeroengine Congress & Exposition, ASME, 2004, GT-2004-53339, Vienna, Austria.
[21] M. Brandt, W. Polifke, P. Flohr, Approximation of joint PDFs by discrete distributions generated with Monte-Carlo methods, Combustion Theory and Modelling 10 (2006) 535–558.
[22] C. Pierce, P. Moin, Progress-variable approach for large-eddy simulation of turbulent combustion (Tech. Report CTR) (2001).
[23] C. Pierce, P. Moin, Progress-variable approach for large-eddy simulation of non-premixed turbulent combustion, Journal of Fluid Mechanics 504 (1) (2004) 73–97.
[24] L. Vervisch, R. Hauguel, P. Domingo, M. Rullaud, Three facets of turbulent combustion modelling: DNS of premixed v-flame, LES of lifted nonpremixed flame and RANS of jet-flame, Journal of Turbulence 5 (2004) 1–36.
[25] P. Domingo, L. Vervisch, B. K., Partially premixed flamelets in LES of nonpremixed turbulent combustion, Combustion Theory and Modelling 6 (4) (2002) 529–551.
[26] P. Domingo, L. Vervisch, D. Veynante, Large-eddy simulation of a lifted methane jet flame in a vitiated coflow, Combustion and Flame 152 (2008) 415–432.
[27] L. Valino, A field monte carlo formulation for calculating the probability density function of a single scalar in a turbulent flow, Flow, Turbulence and Combustion 60 (2) (1998) 157–172.
[28] R. Kulkarni, W. Polifke, Large eddy simulation of auto-ignition in a turbulent hydrogen jet flame using a progress variable approach, Journal of Combustion 2012 (2012) 1–11 (Article ID 780370).
[29] D.G. Goodwin, Cantera: Object-oriented software for reacting flows, california institute of technology, Tech. repweb site, http://blue.caltech.edu/cantera/index.html 2002.
[30] V. Sabelnikov, O. Soulard, Rapidly decorrelating velocity-field model as a tool for solving one-point fokker-planck equations for probability density functions of turbulent reactive scalars, Physical Review E 72 (2005) 016301–016322.
[31] W. Jones, S. Navarro-Martinez, O. Röhl, Large eddy simulation of hydrogen auto-ignition with a probability density function method, Proceedings of the Combustion Institute 31 (2) (2007) 1765–1771.
[32] W. Jones, S. Navarro-Martinez, Large eddy simulation of autoignition with a subgrid probability density function method, Combustion and Flame 150 (2007) 170–187.
[33] W. Jones, S. Navarro-Martinez, Study of hydrogen auto-ignition in a turbulent air co-flow using a large eddy simulation approach, Computers and Fluids 37 (2008) 802–808.
[34] W. Jones, S. Prasad, Large eddy simulation of piloted methane jet flame with high levels of extinction (sandia flame e) using eulerian stochastic fields method, Proceedings of the Combustion Institute (2009).
[35] E. Mastorakos, T. Baritaud, P. T.J., Numerical simulations of autoignition in turbulent mixing flows, Combustion and Flame 109 (1997) 198–223.
[36] S. Sreedhara, K.N. Lakshmisha, Direct numerical simulation of scalar mixing and autoignition in a turbulent medium, Journal of Aeronautical Society of India 53 (2) (2001) 65.
[37] S. Pope, Ten questions concerning the large-eddy simulation of turbulent flows, New Journal of Physics 6 (2004) 35.
[38] I. Celik, Z. Cehreli, I. Yavuz, Index of resolution quality for large eddy simulations, Journal of Fluid Engineering 127 (2005) 949–958.
[39] S. Kerkemeier, C. Frouzakis, K. Boulouchos, E. Mastorakos, Numerical simulation of autoignition of a diluted hydrogen plume in co-flowing turbulent hot air, In: AIAA Aerospace Sciences Meeting Including the New Horizons Forum and Aerospace Exposition, 2010.